CrossMark

ORIGINAL ARTICLE

# Biomechanical performance of retrograde nail for supracondylar fractures stabilization

Nattapon Chantarapanich[1] · Kriskrai Sitthiseripratip[2] · Banchong Mahaisavariya[3] ·
Pongwit Siribodhi[4]

**Abstract** The study compared the biomechanical performance of retrograde nail used to stabilize supracondylar fracture (three different levels) by means of finite element analysis. Three different nail lengths (200, 260, and 300 mm) of stainless steel and titanium nails were under consideration. Intact femur model was reconstructed from Digital Imaging and Communications in Medicine images of Thai cadaveric femur scanned by computed tomography spiral scanner, whereas geometry of retrograde nail was reconstructed with the data obtained from three-dimensional laser scanner. The retrograde nail was virtually attached to the femur before nodes and elements were generated for finite element model. The finite element models were analyzed in two stages, the early stage of fracture healing and the stage after fracture healing. The finding indicated that purchasing proximal locking screw in the bowing region of the femur may be at risk due to the high stresses at the implant and bone. There were no differences in stress level, elastic strain at a fracture gap, and bone stress between stainless steel and titanium implant. Since the intramedullary canal requires reaming to accommodate the retrograde nail, the length of retrograde nail should be as long as necessary. However, in case that the retrograde nail can be accommodated into the intramedullary canal without reaming, the longer retrograde nail can be used.

## 1 Introduction

Supracondylar femur fractures are commonly caused by high-energy trauma impact to the distal femur [21, 27]. The incidence of distal femur fracture is 3 % of femoral fractures and 0.4 % of all fracture [10]. Retrograde nailing technique is one of several efficient techniques to manage the supracondylar fracture as reported by many literatures [11–13, 18, 20, 22–24, 26]. Comparing to the plate fixation technique, the retrograde nailing technique requires less soft tissue dissection, which subsequently decreased blood loss [20]. Although the retrograde nailing technique provides advantages to patients, however, various clinical complications related to the retrograde nail have been reported, for example, non-union [11], loss of reduction [13], knee pain [11], and failure of fixation devices [12, 13, 22, 29, 33]. Among various clinical complications, the one that involving the mechanical failure has been considered, since it can lead the occurrence of other biological complications and it also requires re-operation. Screw breakage, locking screws deflection, and the failure of retrograde nail are common problems. These failures are motivated by high stress concentration such as quadriceps exercise [32].

Many studies showed the experiments on observing the failure of retrograde nail experimentally and numerically. For example, Cheung et al. [6] analyzed the biomechanical

✉ Kriskrai Sitthiseripratip
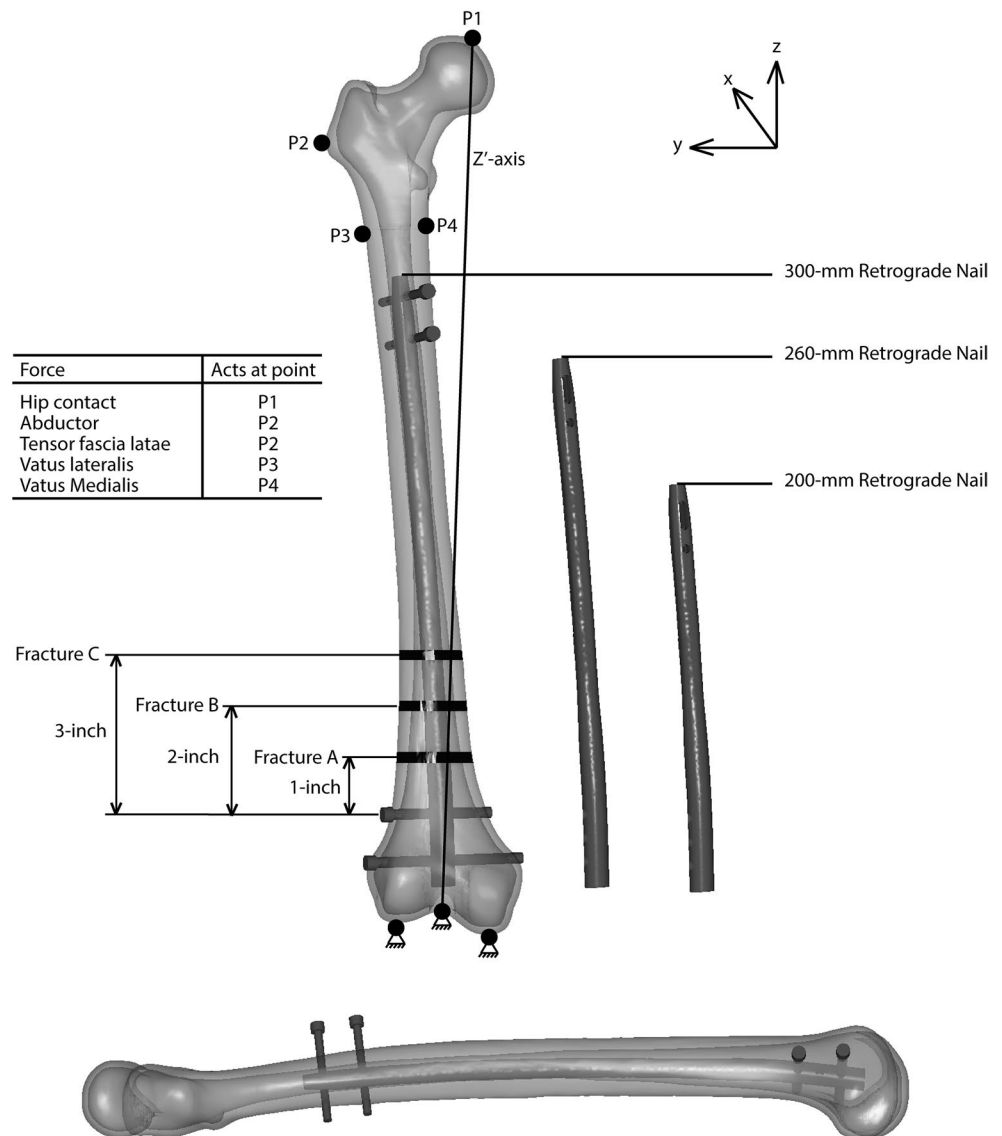    kriskrs@mtec.or.th

1   Department of Mechanical Engineering, Faculty
    of Engineering at Sriracha, Kasetsart University, Sriracha,
    Chonburi, Thailand

2   National Metal and Materials Technology Center (MTEC),
    114 Thailand Science Park, Pahonyothin Road, Klong Luang,
    Pathumthani, Thailand

3   Department of Orthopaedic Surgery and Rehabilitation,
    Faculty of Medicine Siriraj Hospital, Mahidol University,
    Bangkok, Thailand

4   Department of Aerospace Engineering, Faculty
    of Engineering, Kasetsart University, Bangkok, Thailand

**Fig. 1** Loading condition for preclinical testing and boundary conditions of the finite element model

| Force | Acts at point |
|---|---|
| Hip contact | P1 |
| Abductor | P2 |
| Tensor fascia latae | P2 |
| Vatus lateralis | P3 |
| Vatus Medialis | P4 |

performance of the retrograde nail subjected to gait load. Shih et al. [28] investigated the influence of muscle forces relating to failure of distal screw hole at the retrograde nail and locking screws. Chen et al. [4] performed the analysis of biomechanical performance of various retrograde nail models used in distal femur fracture fixation. More recently, Chen et al. [5] compared the performance of retrograde nail with and without an intramedullary allograft for distal femur fracture. However, no report was raised the issue the risk of implant failure or bone secondary fracture due to the effect of location of proximal screw purchasing, which may occur from improper selection of length of retrograde nail.

Geometry of femur presents an anterior bow. Mid-shaft region of femur at about the point which proximal shaft meets distal shaft axes could produce the high stress due to the compression loading. Due to the fact that, purchasing

**Table 1** Materials' properties used in the finite element models [7, 34]

| Region | Elastic modulus (MPa) | Poisson's ratio |
|---|---|---|
| *Cortical bone* | | |
| 1. Femoral neck cortex | 2000 | 0.30 |
| 2. Femoral cortex | 17,000 | 0.28 |
| *Cancellous bone* | | |
| 3. Femoral head | 600 | 0.30 |
| 4. Femoral neck | 1000 | 0.30 |
| 5. Femur | 600 | 0.30 |
| *Fracture region* (*early stage of fracture fixation*) | | |
| 6. Initial connective tissue | 3 | 0.4 |
| *Retrograde nail and locking screws* | | |
| 7. Stainless steel | 2,00,000 | 0.30 |
| 8. Titanium alloy | 1,10,000 | 0.33 |

**Table 2** Loading condition under walking activity [1]

| Force | Early stage of fracture fixation | | | Stage of after fracture healing | | | Acting Location |
|---|---|---|---|---|---|---|---|
| | x | y | z | x | y | z | |
| Hip contact | 115.1 | 230.2 | −921.1 | 225.7 | 451.4 | −1806 | P1 |
| Abductor | 0 | −468 | 694 | 0 | −468 | 694 | P2 |
| Tensor fasciae latae | 158.8 | 117 | −75.2 | 158.8 | 117 | −75.2 | P2 |
| Vastus lateralis | −108 | 8.4 | −543 | −108 | 8.4 | −543 | P3 |
| Vastus medialis | −33.4 | 8.4 | −167 | −33.4 | 8.4 | −167 | P4 |

the locking screws into the cortical bone reduce bone volume which subsequently affects to the bone strength, consequently, purchasing proximal locking screws of retrograde nail around the mid-shaft region where the high stress occurs, this may increase risk of bone fracture and implant failure. Selecting proper retrograde nail length is then considerable to avoid such the motioned risks. This brings objectives for this study to find the safe zone for purchasing the proximal locking screw which then corresponding to the length of the retrograde nail.

This study used the finite element (FE) methods to evaluate the risk of implant failure and bone secondary fracture in the early stage of fracture fixation and in the stage of after fracture healing. The investigation included three different fractures sites located in supracondylar region. The formulation of fracture sites was based on the professional experience in trauma fracture fixation of the author#3. The retrograde nail models used in the study included the length of 200, 260, and 300 mm. The influence of stainless steel and titanium materials on the biomechanical performance of retrograde nail and bone was also investigated. The results from this study were expected to raise the awareness of surgeons for selecting the retrograde nail in managing the supracondylar fracture to prevent mechanical failure of implant and bone secondary fracture during healing period.

## 2 Materials and methods

All presented FE models were constructed using the computer-aided design (CAD) reverse engineering combined with medical imaging techniques based on the data obtained from computed tomography. The analysis was performed using the FE software package (MSC Marc Mentat 2005, MSC Software, Inc., USA).

The considered FE cases included the femur with three different distal fracture locations. Each location was stabilized with three different lengths of retrograde nail. Stainless steel and titanium alloy were given to the retrograde nail to investigate the material influences on the biomechanical performance. Two biological stages were carried out:

1. The early stage of fracture fixation and the stage after fracture healing: it was investigated to observe the implant stress during the critical period which the retrograde nail must be able to withstand the physiological loads.
2. The stage after fracture healing: it was investigated to observe the effect of long term retaining the implant in the body.

Combination of these given conditions produced 36 FE cases.

### 2.1 Finite element model

A Thai male cadaveric femur with unknown age at the time of death was used in the study. Length of the cadaveric femur is 433 mm. The cadaveric femur was scanned with a spiral computed tomography (CT) scanner to obtain the shape of the femur. In epiphysis region of the femur, the scan was performed with 3.0 mm slice thickness, whereas in metaphysis of the femur, the scan was performed with 5.0 mm slice thickness. After scanning, a set of CT image written in Digital Imaging and Communications in Medicine (DICOM) file format was imported into the image processing software package (Mimics, Materialise NV, Belgium). In the software, the three-dimensional CAD femur model was reconstructed by selecting the interested region. Retrograde nails (Zimmer Inc.) employed in this study were acquired the three-dimensional geometry with Kreon Zephyr (KZ50) laser scanner system. All retrograde nails had the distal diameter of 12 mm and shaft diameter of 10 mm. Three lengths of the retrograde nail included in this study were 200, 260, and 300 mm. The retrograde nail had two distal and two proximal transverse screws. The retrograde nail was virtually inserted into the intramedullary canal by aligning the nail axis to the femoral axis. Distal fractures of the femur modeled in this study were transverse-type. Gap of the fracture site was 5 mm. Locations of the distal fracture were 1-inch (Level A), 2-inch (Level B), and 3-inch (Level C) proximal to the distal screw, respectively. Figure 1 shows the femur with distal fractures stabilized by three different retrograde nails.

**Fig. 2** Convergence test in term of von Mises stress

von Mises stress (MPa)



Number of Element
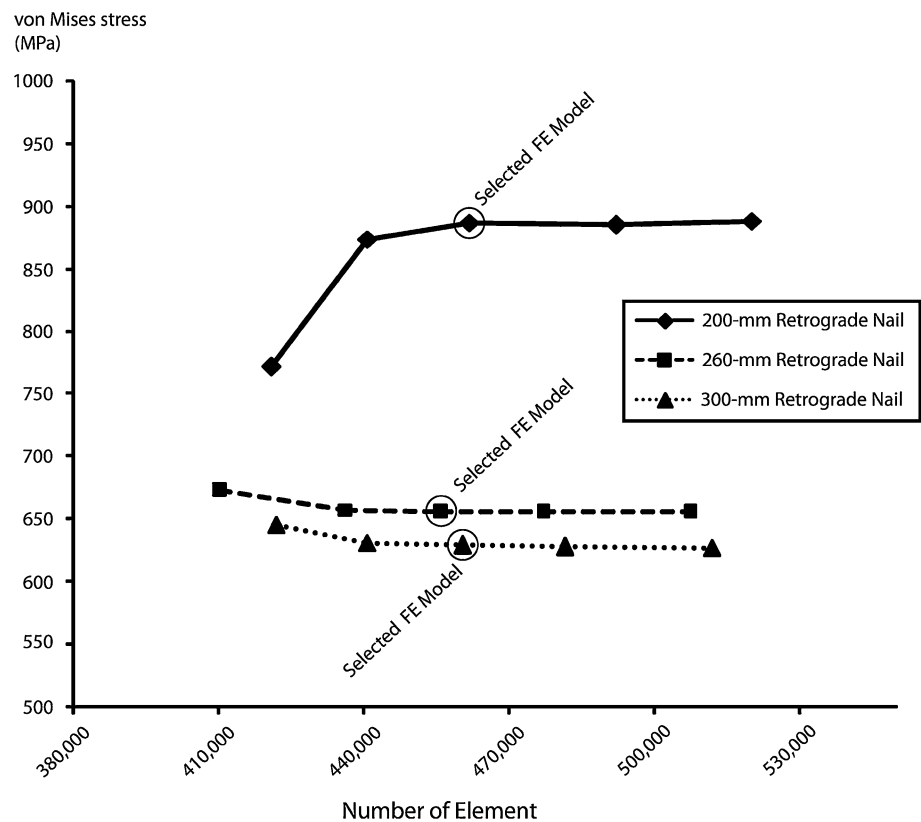
FE models for the femur and the retrograde nails were built up from four-noded tetrahedral elements. The elements were generated with automatic mesh generation technique (Magics RP, Materialise N.V., Belgium).

## 2.2 Material properties

Material properties assigned to all regions of the FE models were homogenous, isotropic, and linearly elastic. Since this work aimed to compare the biomechanical performance of retrograde nails based on similar loading conditions, the material property of the initial connective tissue was then assigned as isotropic to simplify FE computation, although the mechanical behavior of initial connective tissue can be modeled as hyperelastic materials as Mooney–Rivlin. The corresponding material properties shown in Table 1 were attributed to the FE models.

The material properties at the fracture site assigned in the early stage of fracture fixation were initial connective tissue, whereas the material properties at the fracture site in the stage after fracture healing were femoral cortex. Properties of stainless steel and titanium alloy were assigned to the retrograde nail for investigating the influence of two different implant materials.
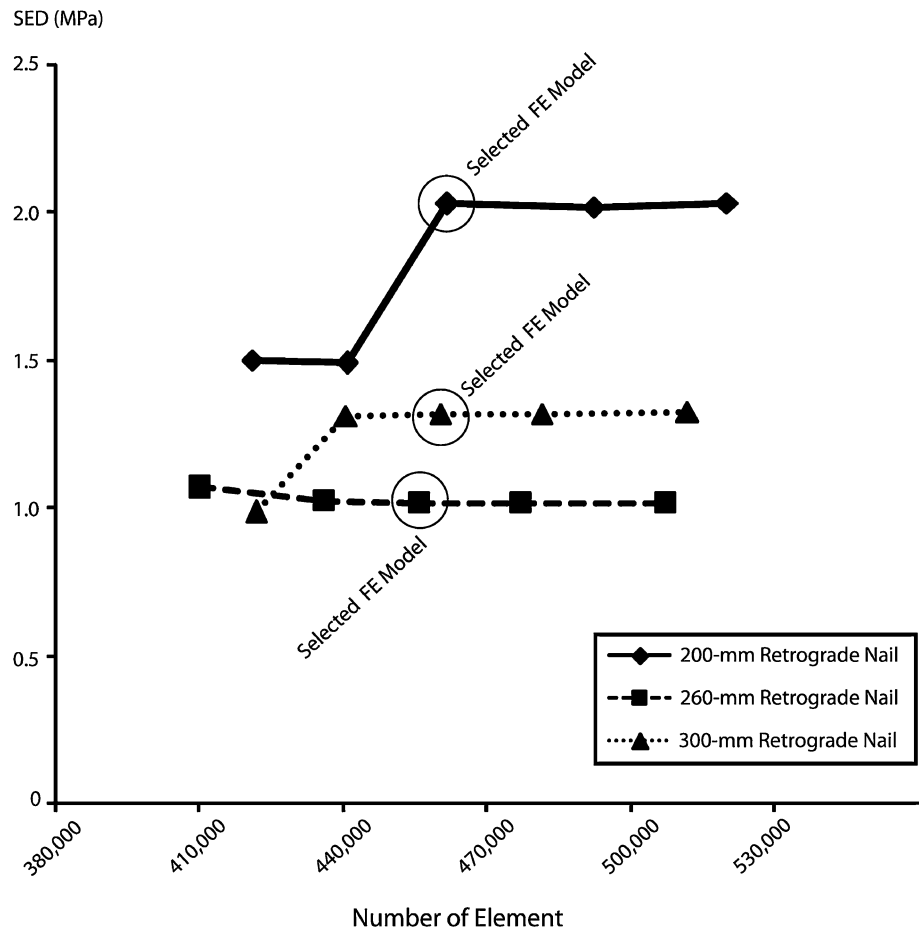
## 2.3 Boundary conditions

The biomechanical forces at 25 percents of gait cycles were applied to the FE models [1]. This is because the forces reached the maximum during entire gait cycle at this stage and was suggested by Heller et al. [15] for preclinical study. The 51 percent of hip contact force was applied in the early stage of fracture fixation, since full-weight bearing is not immediately allowed after the postoperative [19]. The full-weight bearing was then used in the analysis stage after fracture healing. Table 2 shows values of the applied loads.

Physiologically based boundary conditions were used to constrain the femur model [31]. A node at knee joint center was constrained in three translational degrees of freedom. A node at hip contact was constrained in such a way that the hip could only deflect along a hip joint-to-knee joint axis. Figure 1 shows forces and constrained boundary conditions employed in this study.

## 2.4 Contact condition

Frictional contact conditions were also included in the FE models. Friction coefficients of stainless steel/stainless steel, stainless steel/femur, titanium/titanium, and titanium/

**Fig. 3** Convergence test in terms of SED



Figure 3: Convergence test plot showing SED (MPa) versus Number of Element for 200-mm, 260-mm, and 300-mm Retrograde Nail cases, with "Selected FE Model" points circled.

**Table 3** Number of element and corresponding node for FE analysis

| Cases | Number of element | Number of node |
|---|---|---|
| 300-mm retrograde nail | 460,377 | 103,544 |
| 260-mm retrograde nail | 455,925 | 102,483 |
| 200-mm retrograde nail | 461,826 | 104,086 |

femur were 0.15 [17], 0.23 [3], 0.30 [9], and 0.36 [25], respectively. The threads of locking screws were omitted to simplify FE analysis, then the locking screws were bonded to the femur as representation of screw purchasing. The retrograde nail was allowed to displace relatively to the intramedullary canal and distal locking screw.

## 2.5 Element convergence

The numbers of element and node of the FE models were determined by a convergence test in terms of von Mises stress, and strain energy density (SED). Five different numbers of elements were generated for 200-, 260-, and 300-mm retrograde nail cases. The bone material properties assigned to the FE model used for convergence test

were described as shown in Table 1, whereas the material property for retrograde nail and locking screws was stainless steel. Boundary conditions used in the analysis were according to Sect. 2.3. The least numbers of element that the von Mises stress and SED were not affected by changing the numbers of element were selected as FE models.

## 3 Result

### 3.1 FE model validation

Figures 2 and 3 show the convergence test results. For each case, the element size and corresponding number of node that used for further FE analysis were presented in Table 3. In addition, Fig. 4 shows appearance of one of the converged FE model.

### 3.2 Stress distribution at the retrograde nails

Risk of implant failure can be evaluated using von Mises stress. Table 4 shows the maximum equivalent von Mises stress in the implant for each condition. As shown in Figs. 5

### 3.3 Elastic strain

Elastic strain was used to evaluate stability of the fracture sites; the low elastic strain implies the good fracture stability. Table 5 shows the elastic strain in the fracture sites. The elastic strain of fracture sites stabilized with the stainless steel implants was lower than the titanium ones. The shorter implant produced lower value of elastic strain. Different fracture locations stabilized with similar retrograde nail affected slightly on the elastic strain values. At the stage after fracture healing, the elastic strain reduced significantly to lower values. However, the elastic strain was increased slightly after the implant removal.

### 3.4 Bone stress

The maximum bone von Mises stress was observed around the proximal bone/locking screw interface, as shown in Fig. 7. From Table 6, the high values of bone von Mises stresses were observed in the 200-mm retrograde nail cases, for both stainless steel and titanium alloy implants. The lower bone von Mises stresses were found in case that the fractures stabilized with the 260- and 300-mm retrograde nails. During the early stage of fracture fixation, bone von Mises stress in the titanium alloys retrograde nails cases was higher than in the stainless steel cases. After fractures were healed, the bone von Mises stresses reduced. In addition, after the implant removals, the bone stresses were still in low value.

## 4 Discussion

The physiological loading condition at various stages of gait cycle has been applied in previous studies [1, 6, 14] to evaluate the biomedical performance in various parts of human bodies as well as the orthopedic implants using FE method. The FE method allows the experiment to be performed virtually. The FE method would provide accurate result if the definitions of geometry, boundary conditions, and materials properties assigned to the FE model are close to reality. Apart from FE method, the reconstruction of three-dimensional femur model with the CT scanner is considered to be a good technique to obtain the external shape of femur as well as its intramedullary canal geometry without destructive the specimens. Biomechanical analysis of retrograde nails used in stabilizing the supracondylar fractures was analyzed based on these technologies.

The FE results indicate that the maximum implant stress occurs around the retrograde nail/locking screw interface, as also shown in the previous reports [4, 6]. High stress at retrograde nail/locking screw interface can lead to proximal screws and distal screws breakage. The FE results in this



**Fig. 4** Appearance of one of the converged FE model

and 6, the retrograde nails exhibited high von Mises stress at the middle of the retrograde nails as well as around locking screws and the retrograde nail contacts. Different length of the retrograde nails produced different level of the von Mises stress. 260- and 300-mm retrograde nails exhibited the von Mises stress around 594.76–691.36 MPa, whereas 200-mm retrograde nail, the von Mises stress raised up between 730.52 and 887.14 MPa. However, different fracture locations stabilized with identical retrograde nail had little effect on variation of implant von Mises stress. The stainless steel retrograde nails produced the higher von Mises stress than titanium alloy ones. In addition, the implant von Mises stress was reduced to lower magnitudes in the stage after fracture healing.

**Table 4** Equivalent von Mises stress in the implant (MPa)

| Fracture location | Retrograde nail length | Early stage of fracture fixation | | Stage of after fracture healing | |
|---|---|---|---|---|---|
| | | Stainless steel implant | Titanium implant | Stainless steel implant | Titanium implant |
| Fracture A (1-inch) | 300 | 628.63 | 594.76 | 202.97 | 199.08 |
| | 260 | 655.29 | 616.02 | 231.02 | 199.08 |
| | 200 | 887.41 | 730.52 | 199.10 | 199.08 |
| Fracture B (2-inch) | 300 | 654.20 | 636.10 | 202.97 | 199.08 |
| | 260 | 691.36 | 674.73 | 231.02 | 199.08 |
| | 200 | 810.05 | 785.45 | 199.10 | 199.08 |
| Fracture C (3-inch) | 300 | 640.57 | 619.98 | 202.97 | 199.08 |
| | 260 | 670.68 | 628.73 | 231.02 | 199.08 |
| | 200 | 854.50 | 798.45 | 199.10 | 199.08 |

study are relevant to the clinical many reports, for example, clinical reports of proximal screws breakage of Handolin et al. [13], and clinical reports of distal locking screws breakage of Martínez et al. [22], Gynning et al. [12], and Watanabe et al. [33].

In order to find the proper implant for supracondylar fracture stabilization, the percentage of difference was employed to compare how different the maximum von Mises stress exhibited on implants and elastic strain at fracture gap are. Basically, the percentage of difference is defined as difference between two values divided by average of the two values. Table 7 show the percentage difference among von Mises stress of implant with different lengths and materials, and Table 8 shows elastic strain at fracture gap stabilized by implant with different lengths and materials.

From Table 7, slight difference between maximum exhibited von Mises stress of stainless steel and titanium implant was observed for most of the cases. Different fracture levels stabilized with similar implants presented no significant difference on von Mises stress level, and supracondylar fracture sites have no influence on the implant stress.

Maximum von Mises stress exhibited on 200-mm retrograde nail raised to the higher magnitude compared to 260- and 300-mm retrograde nail, as can be seen from the large percentage difference in Table 7 (bold and italic numeric shown in the Table 7). Reason for such a high stress exhibited on 200-mm retrograde nail is from the position of proximal locking screws which were purchased close to the bowing region of the femur. Geometry of femur is anterior bowing. When the loads act on the femur, the stress level at the bowing region is higher than the other regions.

Maximum von Mises stress of 200-mm stainless steel implant also reached beyond the yield stress of material, which typical yield stress for stainless steel ranges from 750 to 960 MPa [30]. Although the maximum von Mises stress exhibited on the 200-mm titanium retrograde nails is below the yield stress of titanium alloy, which is 800–900 MPa, the values were less than the yield point only 0.19–8.69 %. Hence, use of the 200-mm retrograde nail stabilizing in any supracondylar fracture site may increase risk of implant breakage.
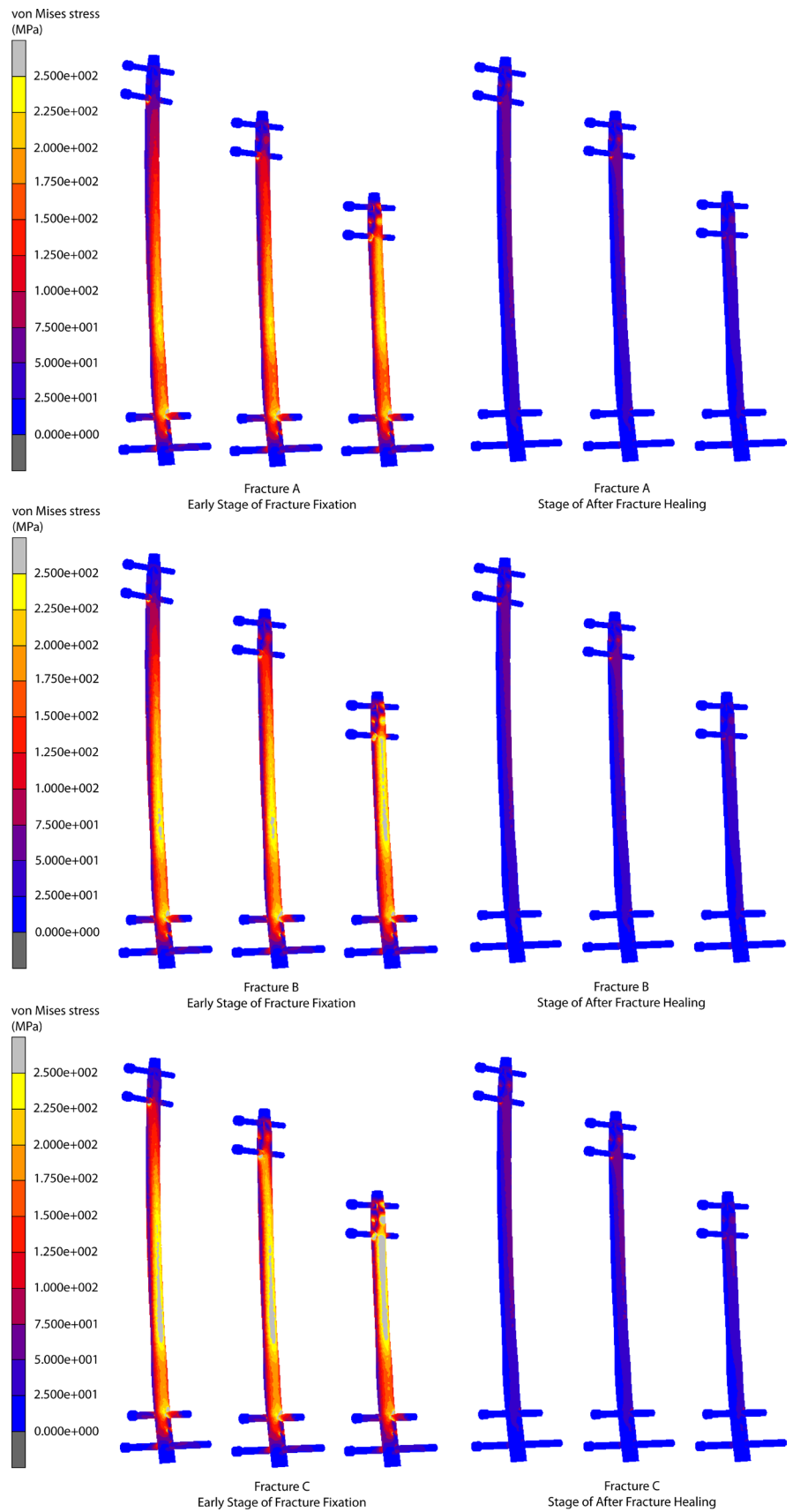
Stress levels for stainless steel and titanium alloys which will be failed by fatigue are 200–350 and 550–700 MPa [30], respectively. For the stress level in the stage after fracture healing, all of stresses exhibiting in the retrograde nails reduced to low values and were below the fatigue failure stresses. The implant may retain within the femur without the risk of failure after fracture is completely healed.

The elastic strain is a parameter used to indicate the fracture stability. Low elastic strain value implies good fracture stability, whereas the high one implies poor fracture stability. In Table 8, it can be observed that the large differences in elastic strain are found between stainless steel and titanium implants (bold and italic numeric in shaded area shown in the Table 8).

Since titanium implant produced the value of elastic strain higher than stainless steel implant, titanium retrograde nails lead to lower fracture stability than those stainless steel retrograde nails do. This can be explained that titanium alloy is softer than stainless steel due to the lower elastic modulus, resulting in the higher deformity of materials, greater movement of fracture site.

For bone stress, the high values of von Mises stress were observed particularly in 200-mm stainless steel and titanium alloys. This is because the proximal locking screws of the 200-mm screws purchased at the bowing region of the femur, which are high stress region. Adult yield stress of the femur is 122.3 MPa [8], and most bone stress producing from 200-mm retrograde nails is over the bone yield stress. It is therefore undesirable to stabilize the supracondylar fracture with the 200-mm retrograde nail.

**Fig. 5** The stress distribution of stainless steel retrograde nail



Fracture A
Early Stage of Fracture Fixation

Fracture A
Stage of After Fracture Healing

Fracture B
Early Stage of Fracture Fixation

Fracture B
Stage of After Fracture Healing

Fracture C
Early Stage of Fracture Fixation

Fracture C
Stage of After Fracture Healing

**Fig. 6** The stress distribution of titanium retrograde nail
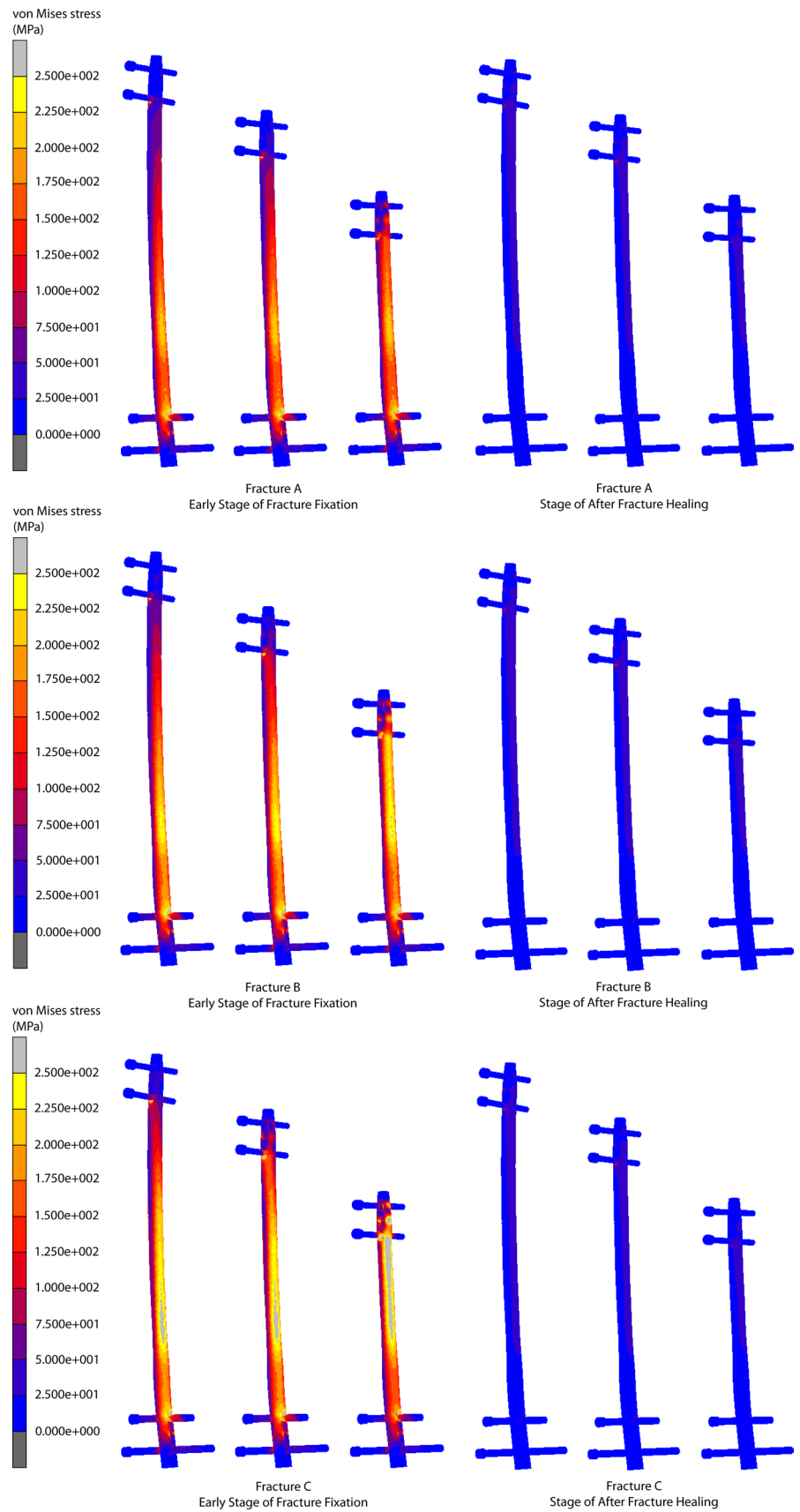
**Table 5** Elastic strain in the fracture zone (μstrain)

| Fracture location | Retrograde nail length | Early stage of fracture fixation | | After fracture healing | | |
|---|---|---|---|---|---|---|
| | | Stainless steel implant | Titanium implant | Stainless steel implant | Titanium implant | After implant removal |
| Fracture A (1-inch) | 300 | 228.54 | 317.02 | 0.63 | 0.69 | 0.96 |
| | 260 | 224.02 | 311.60 | 0.62 | 0.68 | 0.96 |
| | 200 | 205.54 | 303.16 | 0.63 | 0.68 | 0.96 |
| Fracture B (2-inch) | 300 | 247.67 | 367.63 | 0.60 | 0.66 | 0.86 |
| | 260 | 245.79 | 358.55 | 0.60 | 0.65 | 0.86 |
| | 200 | 193.96 | 303.27 | 0.61 | 0.66 | 0.86 |
| Fracture C (3-inch) | 300 | 240.67 | 374.00 | 0.72 | 0.78 | 0.85 |
| | 260 | 229.87 | 352.12 | 0.72 | 0.78 | 0.85 |
| | 200 | 151.24 | 250.15 | 0.72 | 0.78 | 0.84 |
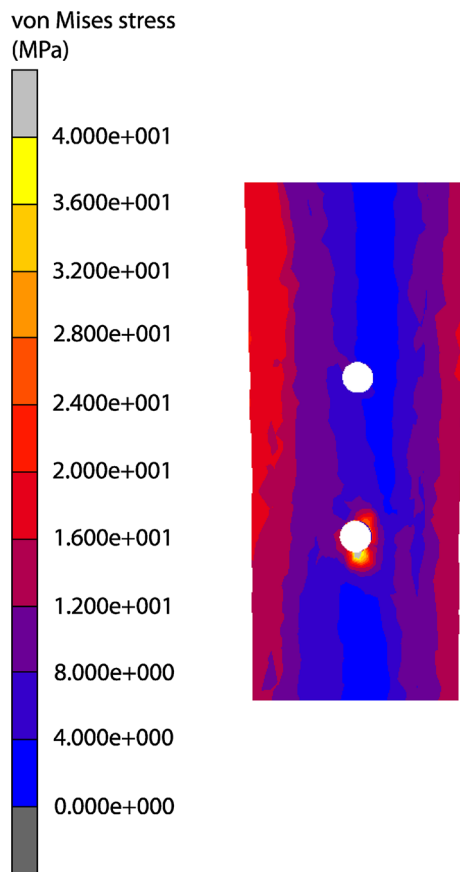


**Fig. 7** Bone stress around the bone–screw interface during the early stage of fracture fixation, fracture A was stabilized by 300 mm length of stainless steel implant

The proximal screws of retrograde nail used for stabilizing the supracondylar fracture should avoid purchasing around the bowing region of femur in order to evade implant failure and bone secondary fracture. Selection of retrograde nail length should depend on the length of femur. Since bowing region of the femur is approximately half of the femur length, the retrograde nail length should be over half of the femur length.

In addition, previous work of Chantarapanich et al. [2] found that most of the cadaveric femora presented the high degree of retrograde nails' mismatching, which the curvature radius of the intramedullary canal could not compensate to the one of the retrograde nail. The intramedullary canal requires extensive reaming to accommodate the retrograde nail insertion. The amount of cortical bone removal also corresponds with the bone strength weakening [16]. Consequently, the longer retrograde nail requires higher amount of cortical bone removal than the shorter one. Selection of the retrograde nail also depends on the morphology of intramedullary canal, i.e., its diameter. If the intramedullary canal is narrow, for example, in healthy adult bone, the length of retrograde nail should be as long as necessary. The excessive bone reaming for unnecessary nail length results in bone weakening. On the other hand, if the intramedullary canal of the femur is large and no additional reaming required, the long retrograde nail can also be used. Although the intramedullary canal of the femur is large enough to accommodate the long retrograde nail, purchasing locking screws in subtrochanteric region is at risk. Diameter of femoral cortical bone around sub-trochanteric region is the least compared with other regions. Purchasing the proximal locking screws requires drilling into cortical bone, certain amount of bone is removed. The bone reduces its strength which may lead to secondary fracture in the sub-trochanteric region.

The results from this investigation rise awareness for the surgeon in terms of selecting the proper length of the retrograde nail, since purchasing the screw around the bowing region of the femur may raise the bone stress at the proximal screw holes beyond the yield stress. This could produce secondary fracture.

**Table 6** Bone equivalent von Mises stress (MPa)

| Fracture location | Retrograde nail length | Early stage of fracture fixation | | After fracture healing | | |
|---|---|---|---|---|---|---|
| | | Stainless steel implant | Titanium implant | Stainless steel implant | Titanium implant | After implant removal |
| Fracture A (1-inch) | 300 | 73.95 | 104.46 | 34.94 | 31.34 | 32.61 |
| | 260 | 58.31 | 62.51 | 40.04 | 38.03 | 29.35 |
| | 200 | 109.98 | 122.70 | 47.73 | 39.75 | 34.66 |
| Fracture B (2-inch) | 300 | 73.65 | 98.33 | 34.94 | 31.34 | 32.61 |
| | 260 | 67.49 | 74.05 | 40.04 | 38.03 | 29.35 |
| | 200 | 127.63 | 157.69 | 47.73 | 39.75 | 34.66 |
| Fracture C (3-inch) | 300 | 70.54 | 92.04 | 34.94 | 31.34 | 32.61 |
| | 260 | 81.29 | 98.04 | 40.04 | 38.03 | 29.35 |
| | 200 | 149.12 | 195.68 | 47.73 | 39.75 | 34.66 |

## 5 Conclusion

This study investigated the biomechanical performance of retrograde nail used for stabilizing supracondylar fracture by means of FE method. The FE model of the intact femur and the retrograde nails was reconstructed using the reverse engineering technique. The material properties assigned to various portions of FE model were homogenous, isotropic, and linearly elastic. Three supracondylar fracture sites stabilized with three different lengths of stainless steel and titanium alloy retrograde nails were carried out. The FE analyses included two stages: the early stage of fracture healing and the stage after fracture healing.

The use of fixation in the early stage of fracture healing was critical. The stress level at the implant and bone at the early stage of fracture healing was higher than that in the stage after fracture healing. The fracture stability at the early stage of fracture healing was lower than the stage after fracture healing. The implant can be retained in the stage after fracture healing due to the stress level exhibited on the implant was below the fatigue failure stress level.

**Table 7** Percentage difference among von Mises stress of implants with different lengths and materials

| | | 300-mm Stainless steel | | | 260-mm Stainless steel | | | 200-mm Stainless steel | | | 300-mm Titanium | | | 260-mm Titanium | | | 200-mm Titanium | | | | |
|---|---|---|---|---|---|---|---|---|---|---|---|---|---|---|---|---|---|---|---|---|---|---|
| | | A | B | C | A | B | C | A | B | C | A | B | C | A | B | C | A | B | C | | |
| 300-mm Stainless steel | A | ■ | 1.0 | 0.5 | 1.0 | 2.4 | 1.6 | 8.5 | 6.3 | 7.6 | 1.4 | 0.3 | 0.3 | 0.5 | 1.8 | 0.0 | 3.7 | 5.5 | 5.9 | A | 300-mm Stainless steel |
| | B | | ■ | 0.5 | 0.0 | 1.4 | 0.6 | 7.6 | 5.2 | 6.6 | 2.4 | 0.7 | 1.3 | 1.5 | 0.8 | 1.0 | 2.8 | 5.3 | 5.0 | B | |
| | C | | | ■ | 0.6 | 1.9 | 1.1 | 8.1 | 5.8 | 7.2 | 1.9 | 0.2 | 0.8 | 1.0 | 1.3 | 0.5 | 3.3 | 5.1 | 5.5 | C | |
| 260-mm Stainless steel | A | | | | ■ | 1.3 | 0.6 | 7.5 | 5.3 | 6.6 | 2.4 | 0.7 | 1.4 | 1.5 | 0.7 | 4.9 | 2.7 | 4.5 | 4.9 | A | 260-mm Stainless steel |
| | B | | | | | ■ | 0.8 | 6.2 | 4.0 | 5.3 | 3.8 | 4.0 | 2.7 | 2.9 | 0.6 | 2.4 | 1.4 | 3.2 | 3.6 | B | |
| | C | | | | | | ■ | 7.0 | 4.7 | 6.0 | 3.0 | 1.3 | 2.0 | 2.1 | 0.2 | 1.6 | 2.1 | 3.9 | 4.3 | C | |
| 200-mm Stainless steel | A | | | | | | | ■ | 2.3 | 0.9 | 9.9 | 8.2 | 8.9 | 9.0 | 6.8 | 8.5 | 4.8 | 3.0 | 2.6 | A | 200-mm Stainless steel |
| | B | | | | | | | | ■ | 1.3 | 7.7 | 6.0 | 6.6 | 6.8 | 4.6 | 6.3 | 2.6 | 0.8 | 0.4 | B | |
| | C | | | | | | | | | ■ | 9.0 | 7.3 | 8.0 | 8.1 | 5.9 | 7.6 | 3.9 | 2.1 | 1.7 | C | |
| 300-mm Titanium | A | | | | | | | | | | ■ | 1.7 | 1.0 | 0.9 | 3.1 | 1.4 | 5.1 | 6.9 | 7.3 | A | 300-mm Titanium |
| | B | | | | | | | | | | | ■ | 0.6 | 0.8 | 1.5 | 0.3 | 3.5 | 5.3 | 5.7 | B | |
| | C | | | | | | | | | | | | ■ | 0.2 | 2.1 | 0.4 | 4.1 | 6.7 | 6.3 | C | |
| 260-mm Titanium | A | | | | | | | | | | | | | ■ | 2.3 | 0.5 | 4.3 | 6.0 | 6.4 | A | 260-mm Titanium |
| | B | | | | | | | | | | | | | | ■ | 1.8 | 2.0 | 3.8 | 4.2 | B | |
| | C | | | | | | | | | | | | | | | ■ | 3.7 | 5.5 | 5.9 | C | |
| 200-mm Titanium | A | | | | | | | | | | | | | | | | ■ | 1.8 | 2.2 | A | 200-mm Titanium |
| | B | | | | | | | | | | | | | | | | | ■ | 4.2 | B | |
| | C | | | | | | | | | | | | | | | | | | ■ | C | |

**Table 8** Percentage difference among elastic strain of fracture gap produced by different lengths and materials

| | | 300-mm Stainless steel | | | 260-mm Stainless steel | | | 200-mm Stainless steel | | | 300-mm Titanium | | | 260-mm Titanium | | | 200-mm Titanium | | | | |
|---|---|---|---|---|---|---|---|---|---|---|---|---|---|---|---|---|---|---|---|---|---|---|
| | | A | B | C | A | B | C | A | B | C | A | B | C | A | B | C | A | B | C | | |
| 300-mm Stainless steel | A | ■ | 2.0 | 1.3 | 0.5 | 1.8 | 0.1 | 2.6 | 4.1 | 10.2 | 8.1 | 11.7 | 12.1 | 7.7 | 11.1 | 10.6 | 7.0 | 7.0 | 2.3 | A | 300-mm Stainless steel |
| | B | | ■ | 0.7 | 2.5 | 0.2 | 1.9 | 4.6 | 6.7 | 12.1 | 6.1 | 9.7 | 10.2 | 5.7 | 9.1 | 8.7 | 5.0 | 4.9 | 0.2 | B | |
| | C | | | ■ | 1.8 | 0.5 | 1.1 | 3.9 | 5.4 | 11.4 | 6.8 | 10.4 | 10.8 | 6.4 | 9.8 | 9.4 | 5.7 | 5.8 | 1.0 | C | |
| 260-mm Stainless steel | A | | | | ■ | 2.3 | 0.6 | 2.2 | 3.6 | 9.7 | 8.6 | 12.1 | 12.5 | 8.2 | 11.5 | 2.8 | 7.5 | 7.5 | 2.8 | A | 260-mm Stainless steel |
| | B | | | | | ■ | 1.7 | 4.5 | 5.9 | 11.9 | 6.3 | 9.9 | 10.3 | 5.9 | 9.3 | 8.9 | 5.2 | 5.2 | 0.4 | B | |
| | C | | | | | | ■ | 2.8 | 4.2 | 10.3 | 8.0 | 11.5 | 11.9 | 7.5 | 10.9 | 10.5 | 6.9 | 6.9 | 2.1 | C | |
| 200-mm Stainless steel | A | | | | | | | ■ | 1.4 | 7.6 | 10.7 | 14.1 | 14.5 | 10.3 | 13.6 | 13.1 | 9.6 | 9.6 | 4.9 | A | 200-mm Stainless steel |
| | B | | | | | | | | ■ | 6.2 | 12.0 | 15.5 | 15.8 | 11.6 | 14.9 | 14.5 | 11.0 | 11.0 | 6.3 | B | |
| | C | | | | | | | | | ■ | 17.7 | 20.9 | 21.2 | 17.3 | 20.3 | 20.0 | 16.7 | 16.7 | 12.3 | C | |
| 300-mm Titanium | A | | | | | | | | | | ■ | 3.7 | 4.1 | 0.4 | 3.1 | 2.6 | 1.1 | 1.1 | 5.9 | A | 300-mm Titanium |
| | B | | | | | | | | | | | ■ | 0.4 | 4.1 | 0.6 | 1.1 | 4.8 | 4.8 | 9.5 | B | |
| | C | | | | | | | | | | | | ■ | 4.6 | 1.1 | 1.5 | 5.2 | 5.2 | 9.9 | C | |
| 260-mm Titanium | A | | | | | | | | | | | | | ■ | 3.5 | 3.1 | 0.7 | 0.7 | 5.5 | A | 260-mm Titanium |
| | B | | | | | | | | | | | | | | ■ | 0.5 | 4.2 | 4.2 | 8.9 | B | |
| | C | | | | | | | | | | | | | | | ■ | 3.7 | 3.7 | 8.5 | C | |
| 200-mm Titanium | A | | | | | | | | | | | | | | | | ■ | 0.0 | 4.8 | A | 200-mm Titanium |
| | B | | | | | | | | | | | | | | | | | ■ | 8.9 | B | |
| | C | | | | | | | | | | | | | | | | | | ■ | C | |

The 200-mm retrograde nail exhibited the higher von Mises stress level than 260- and 300-mm retrograde nails. In any implant materials, the stress level of 200-mm retrograde nails almost reached or exceeded the yield stress of materials. The titanium alloy implant presented the lower stress level than the stainless steel implant. In contrast, it produced the poorer fracture stability than the stainless steel implant. In most cases, the titanium alloys implant presented the high possibility of bone secondary fracture because the bone stress reached the risk level.

Selection of proper retrograde nail length should depend on the femoral length and bone morphology. The length of femoral length for stabilizing supracondylar fracture should be over the bowing region of femur to avoid purchasing the proximal screws close to the high stress region. However, the length of retrograde nail should be lower than the subtrochanteric region. For bone morphology, intramedullary canal diameter is an important factor. Large intramedually canal could compensate well with long retrograde nail, whereas narrow intramedullary canal, the length of retrograde nail should be as long as necessary.

**Compliance with ethical standards**

# References

1. Behrens BA, Nolte I, Wefstaedt P, Stukenborg-Colsman C, Bouguecha A (2009) Numerical investigations on the strain-adaptive bone remodelling in the periprosthetic femur: influence of the boundary conditions. Biomed Eng Online 8(7):1–9
2. Chantarapanich N, Mahaisavariya B, Siribodhi P, Sitthiseripratip K (2011) Geometric mismatch analysis of retrograde nail in the Asian femur. Surg Radiol Anat 33:755–761
3. Chen WP, Tai CL, Shih CH, Hsieh PH, Leou MC, Lee MS (2004) Selection of fixation devices in proximal femur rotational osteotomy: clinical complications and finite element analysis. Clin Biomech 19(3):255–262
4. Chen SH, Yu TC, Chang CH, Lu YC (2008) Biomechanical analysis of retrograde intramedullary nail fixation in distal femoral fractures. Knee 15:384–389
5. Chen SH, Chiang MC, Hung CH, Lin SC, Chang HW (2014) Finite element comparison of retrograde intramedullary nailing and locking plate fixation with/without an intramedullary allograft for distal femur fracture following total knee arthroplasty. Knee 21:224–231
6. Cheung G, Zalzal P, Bhandari M, Spelt JK, Papini M (2004) Finite element analysis of a femoral retrograde intramedullary nail subject to gait loading. Med Eng Phys 26:93–108
7. Claes LE, Heigele CA (1999) Magnitudes of local stress and strain along bony surfaces predict the course and type of fracture healing. J Biomech 32:255–266

8. Currey JD (2004) Tensile yield in compact bone is determined by strain, post-yield behaviour by mineral content. J Biomech 37:549–556

9. Eberle S, Gerber C, von Oldenburg G, Hungerer S, Augat P (2009) Type of hip fracture determines load share in intramedullary osteosynthesis. Clin Orthop Relat Res 467:1972–1980

10. Ehlinger M, Ducrot G, Adam P, Bonnomet F (2013) Distal femur fractures. Surgical techniques and a review of the literature. Orthop Traumatol Surg Res 99:353–360

11. Gao K, Gao W, Huang J, Li H, Li F, Tao J, Wang Q (2013) Retrograde nailing versus locked plating of extra-articular distal femoral fractures: Comparison of 36 cases. Med Princ Pract 22:161–166

12. Gynning JB, Hansen D (1999) Treatment of distal femoral fractures with intramedullary supracondylar nails in elderly patients. Injury 30:43–46

13. Handolin L, Pajarinen J, Lindahl J, Hirvensalo E (2004) Retrograde intramedullary nailing in distal femoral fractures—results in a series of 46 consecutive operations. Injury 35:517–522

14. Helgason B, Pálsson H, Rúnarsson TP, Frossard L, Viceconti M (2009) Risk of failure during gait for direct skeletal attachment of a femoral prosthesis: a finite element study. Med Eng Phys 31:595–600

15. Heller MO, Bergmann G, Kassi JP, Claes L, Haas NP, Duda GN (2005) Determination of muscle loading at the hip joint for use in pre-clinical testing. J Biomech 38:1155–1163

16. Hipp JA, McBroom RJ, Cheal EJ, Hayes WC (1989) Structural consequences of endosteal metastatic lesions in long bones. J Orthop Res 7:828–837

17. Hrubina M, Horák Z, Bartoška R, Navrátil L, Rosina J (2013) Computational modeling in the prediction of dynamic hip screw failure in proximal femoral fractures. J Appl Biomed 11(3):143–151

18. Kim J, Kang SB, Nam K, Rhee SH, Won JW, Han HS (2012) Retrograde intramedullary nailing for distal femur fracture with osteoporosis. Clin Orthop Surg 4:307–312

19. Koval KJ, Sala DA, Kummer FJ, Zuckerman JD (1998) Postoperative weight-bearing after a fracture of the femoral neck or an intertrochanteric fracture. J Bone Joint Surg Am 80:352–356

20. Kumar A, Jasani V, Butt MS (2000) Management of distal femoral fractures in elderly patients using retrograde titanium supracondylar nails. Injury 31:169–173

21. Martinet O, Cordey J, Harder Y, Maier A, Bühler M, Barraud GE (2000) The epidemiology of fractures of the distal femur. Injury 31:62–63

22. Martínez AA, Pérez JM, Herrera A, Lallana JJ (2000) Unusual complications of supracondylar nails. Injury 31:811–813

23. Melvin JS, Smith JL, Sims SH, Patt JC (2012) The use of an interference fit retrograde nail as an adjunct to plate fixation of a complex Vancouver B1 periprosthetic femoral fracture. Injury 43:1779–1782

24. Metikala S, Mohammed R (2011) Closed retrograde retrieval of the distal broken segment of femoral cannulated intramedullary nail using a ball-tipped guide wire. Indian J Orthop 45:347–350

25. Mischler S, Pax G (2002) Tribological behavior of titanium sliding against bone. Eur Cell Mater 3:28–29

26. Ostrum RF, Maurer JP (2009) Distal third femur fractures treated with retrograde femoral nailing and blocking screws. J Orthop Trauma 23:681–684

27. Schandelmaier P, Partenheimer A, Koenemann B, Grün OA, Krettek C (2001) Distal femoral fractures and LISS stabilization. Injury 32:SC55–SC63

28. Shih KS, Tseng CS, Lee CC, Lin SC (2008) Influence of muscular contractions on the stress analysis of distal femoral interlocking nailing. Clin Biomech 23:38–44

29. Singh SK, El-Gendy KA, Chikkamuniyappa C, Houshian S (2006) The retrograde nail for distal femoral fractures in the elderly: high failure rate of the condyle screw and nut. Injury 37:1004–1010

30. Sitthiseripratip K, Van Oosterwyck H, Vander Sloten J, Mahaisavariya B, Bohez ELJ, Suwanprateeb J, Van Audekercke R, Oris P (2003) Finite element study of trochanteric gamma nail for trochanteric fracture. Med Eng Phys 25:99–106

31. Speirs AD, Heller MO, Duda GN, Taylor WR (2007) Physiologically based boundary conditions in finite element modelling. J Biomech 40:2318–2323

32. Suresh SS (2013) Exchange nailing and percutaneous bone grafting for management of aseptic non-union of the femur. Hard Tissue 2(1):8

33. Watanabe Y, Takai S, Yamashita F, Kusakabe T, Kim W, Hirasawa Y (2002) Second-generation intramedullary supracondylar nail for distal femoral fractures. Int Orthop 26:85–88

34. Wei HW, Sun SS, Jao SHE, Yeh CR, Cheng CK (2005) The influence of mechanical properties of subchondral plate, femoral head and neck on dynamic stress distribution of the articular cartilage. Med Eng Phys 27:295–304

**Nattapon Chantarapanich, Ph.D** is a Faculty member of the Department of Mechanical Engineering, Faculty of Engineering at Sriracha, Kasetsart University, where he has been since 2013. His main research interests are orthopedic biomechanics, orthopedic implant design, and additive manufacturing in medical applications .

**Kriskrai Sitthiseripratip, D.Eng** is a Principal Researcher of the Biomedical Engineering Research Unit at the National Metal and Materials Technology Center (MTEC), where he has been since 2003. He also currently serves as Lab Head of Medical Devices Laboratory. His main research interests are medical device development, medical imaging, and additive manufacturing technologies .

**Banchong Mahaisavariya, M.D** is Senior Vice President and Professor of Orthopaedics at Mahidol University. He is former Dean of the Faculty of Graduate Studies and also a Member of the Mahidol University Council. He has been a Council Member at the Royal College of Orthopaedic Surgeon of Thailand since 1998 where he is currently serving as the President Elected .

**Pongwit Siribodhi, Ph.D** is Associate Professor of Aerospace Engineering at Kasetsart University. His main research interests are aerospace and marine engineering .